Thin Solid Films 596 (2015) 29–33

Contents lists available at ScienceDirect

Thin Solid Films

journal homepage: www.elsevier.com/locate/tsf

Titanium oxynitride thin films as high-capacity and high-rate anode materials for lithium-ion batteries

Kuo-Feng Chiu [a], Shih-Hsuan Su [a,*], Hoang-Jyh Leu [b], Chen-Hsien Hsia [a]

[a] Department of Materials Science and Engineering, Feng Chia University, 100 Wenhwa Rd., Taichung 40724, Taiwan
[b] Master's Program of Green Energy Science and Technology, Feng Chia University, 100 Wenhwa Rd., Taichung 40724, Taiwan

ARTICLE INFO

Article history:
Received 31 March 2015
Received in revised form 8 September 2015
Accepted 11 September 2015
Available online 21 October 2015

Keywords:
TiO_2
TiO_xN_y
Oxynitride
Thin film
Anodes
Lithium ion batteries

ABSTRACT

Titanium oxynitride (TiO_xN_y) was synthesized by reactive magnetron sputtering in a mixed N_2/O_2/Ar gas at ambient temperature. TiO_xN_y thin films with various amounts of nitrogen contents were deposited by varying the N_2/O_2 ratios in the background gas. The synthesized TiO_xN_y films with different compositions ($TiO_{1.837}N_{0.060}$, $TiO_{1.890}N_{0.068}$, $TiO_{1.865}N_{0.073}$, and $TiO_{1.882}N_{0.163}$) all displayed anatase phase, except $TiO_{1.882}N_{0.163}$. The impedances and grain sizes showed obvious variations with the nitrogen contents. A wide potential window from 3.0 V to 0.05 V, high-rate charge–discharge testing, and long cycle testing were applied to investigate the performances of synthesized TiO_xN_y and pure TiO_2 as anodes for lithium-ion batteries. These TiO_xN_y anodes can be cycled under high rates of 125 μA/cm^2 (10 °C) because of the lower charge–transfer resistance compared with the TiO_2 anode. At 10 °C the discharge capacity of the optimal TiO_xN_y composition is 1.5 times higher than that of pure TiO_2. An unexpectedly large reversible capacity of ~300 μAh/cm^2 μm (~800 mAh/g) between 1.0 V and 0.05 V was recorded for the TiO_xN_y anodes. The TiO_xN_y anode was cycled (3.0 V to 0.05 V) at 10 °C over 300 times without capacity fading while delivering a capacity of ~150 μAh/cm^2 μm (~400 mAh/g).

© 2015 Elsevier B.V. All rights reserved.

1. Introduction

Lithium-ion batteries have been the main energy storage devices for consumer electronic products for decades. Recently, the rapid development of plug-in electric vehicles, hybrid electric vehicles, and other high-power applications has demanded improved safety and stability in lithium-ion batteries. TiO_2 is naturally abundant, environmentally friendly, chemically stable, and low-cost. It is considered a safe and stable anode material because the reduction voltage vs. Li/Li^+ (~1.7 V) of the material is relatively high, which avoids the devastating effects of lithium condensation at low cell voltages [1,2]. In addition, TiO_2 is also known as a stress-free anode with good cycle life and low volume expansion during charge–discharge processes, which are great advantages over graphite or alloy-type anode materials [3]. However, for applications in lithium-ion batteries, pure TiO_2 has the drawbacks of low lithium-ion diffusivity (10^{-15}–10^{-9} cm^2 S^{-1}) and low electrical conductivity (10^{-12}–10^{-7} S cm^{-1}) [2], which limit the utility of the material in high-current power sources.

The intrinsically poor rate capability of TiO_2 has also limited practical applications of the material [4]. Much research attention has been devoted to nano-structured materials [4,5], as the decreased lithium-ion diffusion length enhances the rate capability within the anode. Nanostructures also increase the available surface area. It was demonstrated that high surface area correlated to a significant capacitive effect at the electrode/electrolyte interface [6], which increased the high rate capacity.

TiO_xN_y thin films or nano-structures are frequently used in tribology [7–9]. It was reported that high-hardness films could be obtained by optimizing the nitrogen content in the metal nitride films. The technique has also been adopted in the fabrication of thin films for optical and electrical applications [10–12]. TiO_xN_y has been shown to have improved optical absorption and photocatalytic activity compared with TiO_2 [10,11]. It has been demonstrated that TiO_xN_y can be prepared by reactive magnetron sputtering, and the material exhibits a significant absorption capacity for visible light. It was also reported that TiO_xN_y exhibited higher conductivity due to the decrease of band gap with an increase of nitrogen contents [13]. Some attempts at introducing nitrogen into TiO_2 to improve the rate capability have been reported [4,12], but the highest capacity achieved was ~200 mAh/g (cut-off at 1.0 V) at 0.2 °C, while that at 10 °C is less than 50 mAh/g, which leaves room for improvement.

Only a few published papers report on the nitridation with NH_3 of TiO_2 to fabricate TiO_xN_y for lithium-ion battery anodes [4,14]. Nitridated TiO_2 was shown to exhibit both improved cyclability and rate capability compared with TiO_2, attributed to the higher electrochemical stability and elevated conductivity of TiO_xN_y. However, nitridation with NH_3 is a surface modification method with a possible limitation on nitride layer depth. In order to address this issue, reactive sputtering with nitrogen gas was applied in this study. The present paper demonstrates the

* Corresponding author.
E-mail addresses: minimono42@gmail.com, p0043192@fcu.edu.tw (S.-H. Su).

http://dx.doi.org/10.1016/j.tsf.2015.09.083
0040-6090/© 2015 Elsevier B.V. All rights reserved.

in situ nitridation process by sputtering under mixed N_2/O_2 gas. TiO_xN_y films were fabricated by sputter deposition in mixed N_2/O_2/Ar gas. The morphologies and structures of the TiO_xN_y films were systematically characterized as a function of different N_2/O_2/Ar mixing ratios. The low-potential (<1.0 V) electrochemical performances of the TiO_xN_y anodes were investigated to understand the phenomena of over-lithiation for these anodes.

2. Experimental details

TiO_2 and TiO_xN_y thin films were synthesized using radio frequency (RF) magnetron sputter deposition under the operating pressure of 2.0 Pa (base vacuum 4.0×10^{-4} Pa). A pure TiO_2 target (Gredmann Ltd. 99.5%) measuring 2 in. or 50 mm in diameter was used. The RF power of 100 W was applied and the target–substrate distance was 50 mm. The total gas flow rate during the deposition was maintained at 15 sccm, composed of a constant Ar flow of 11 sccm and a mixed N_2/O_2 flow of 4 sccm. Various N_2/O_2 flow ratios of 0/4, 2/2, 3/1, 3.5/0.5, and 4/0 were applied to produce samples denoted as N0, N2, N3, N35, and N4, respectively. The thicknesses of all samples for electrochemical tests were kept at ~100 nm.

The compositions and chemical bindings were characterized using X-ray Photoelectron Spectrometry (XPS, VGS Thermo K-Alpha) with an Al Kα source at the energy of 1486.6 eV. The binding energies for different elements were identified by an XPS database [15]. The X-ray diffraction (XRD, Bruker D8SSS) patterns of the TiO_xN_y thin films were acquired using the grazing-angle diffraction method with Cu Kα radiation (wavelength = 1.5405 Å) scanned from 10 to 50° at a scan rate of 3°/min. The surface morphologies were observed by field emission scanning electron microscopy (FESEM, Hitachi S-4800). The resistances of the TiO_2 and TiO_xN_y films were measured by an Agilent 4338B milliohmmeter, and the conductivities of all samples were derived from the measured resistances.

The films were deposited on stainless steel sheets measuring 13 mm in diameter and packed into coin cells in an Ar-filled glove box for the electrochemical measurements. TiO_xN_y thin films were used as the working electrodes and lithium metal foils were used as the counter and reference electrodes. The electrolyte was 1 M $LiPF_6$ in a 1:2 ethylene carbonate/ethyl methyl carbonate (EC/EMC) solution. Galvanostatic measurements were performed using an electrochemical measurement system (Arbin Instruments, BT-2000). In order to understand the reactions at low potential, the potential window was extended to 0.05 V. The cells were charged and discharged in the range of 3.0–0.05 V (vs. Li/Li^+). Various current densities of 2.5, 12.5, 62.5, and 125 μA/cm^2, corresponding to charge rates of 0.2, 1, 5, and 10 °C, respectively, were applied. The specific volume capacities were calculated by the substrate area and film thickness. The mass capacities were obtained from the theoretical density of TiO_2 and the film volume. The electrochemical impedance spectra (EIS) were analyzed using an impedance spectroscope (HIOKI 3522-50 LCR HiTESTER) over the frequency range from 100 kHz to 100 mHz with 20 mV amplitude.

3. Results and discussion

The XRD patterns of the TiO_xN_y thin films are shown in Fig. 1. Sample N0 exhibits two diffraction peaks near 25° and 48°, which correspond to the (101) and (200) peaks of the anatase TiO_2 phase (JCPDS no. 21-1272) [16]. As the N_2 flows are introduced in the deposition process (samples N2, N3, and N35), the previously mentioned diffraction peaks show no apparent shift and the films remain polycrystalline anatase. No phase transformation occurs for films made with N_2/O_2 ratios lower than 3.5/0.5. By terminating the O_2 flow and increasing the N_2/O_2 ratio to 4/0, the film becomes amorphous or nano-structured with no recorded diffraction peaks, indicating that no crystalline phase can be obtained with high N_2 flow. The amount of N in the N4 sample is twice that of the other samples, whereas the oxygen level is similar among all samples. The amorphous structure may result from the deterioration of the TiO_2 phase by the excessive amount of nitrogen incorporation in the films [17]. It is also possible that the increased nitrogen content decreases the grain sizes in the film, and eventually nano-scale grains are formed [8].The average grain sizes of the deposited thin films were calculated from the full width at half maximum of the (101) peak using the Scherrer equation [16]. The results show grain sizes of 37.2, 36.6, 30.3, and 28.2 nm for samples N0, N2, N3, and N35, respectively. The average sizes decrease with increasing N_2/O_2 ratios, except in sample N4, which exhibits no diffraction peak.

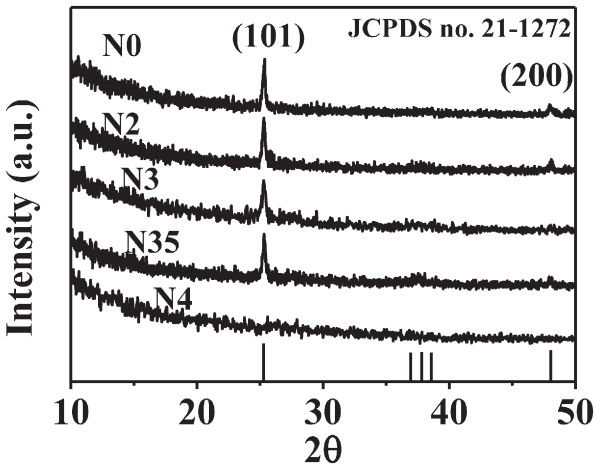

Fig. 1. XRD patterns of TiO_xN_y thin films of N0, N2, N3, N35, and N4.

Fig. 2 contains SEM micrographs of the thin films deposited under different conditions. Sample N0, deposited without N_2, exhibits spindle-like grains with dimensions of ~70 nm in the long axis and ~20 nm in the short axis (Fig. 2(a)), which is the typical grain morphology of sputter-deposited anatase TiO_2 [18]. As the N_2 flow is introduced during deposition (Figs. 2(b)–(e)), the morphologies of the grains become more granular. An obvious decrease in grain size with increasing N_2/O_2 ratio can be clearly observed. The cross-sectional views of all samples exhibit column-like structures, as shown in Fig. 2. The cross-sectional view of sample N4 shows low resolution; therefore, a thicker film of ~300 nm was prepared for observation. The deposition rates for samples N0, N2, N3, and N35, are around 1.0 nm/min, whereas N4 is 2.2 nm/min. Although TiO_2 target was used in this study, the results show the existence of O_2 in the sputtering gas is essential for the formation of anatase phase. Without O_2 flow, no crystalline films can be obtained, and the deposition rate is much higher. The high deposition rate under no O_2 flow (N4) can be attributed to the high oxygen affinity of the TiO_2 target. It has been reported that the deposition rate can abruptly change when sputtering from a TiO_2 target with and without O_2 flow [19]. A slight increase of O_2 flow greatly reduces the deposition rates due to the high oxygen affinity of TiO_2 target.

The XPS spectra of the thin films deposited under various N_2/O_2 ratios were measured. All films deposited under N_2/O_2 flows exhibit both N_{1s} and O_{1s} bands, indicating the successful deposition of TiO_xN_y thin films. For all TiO_xN_y films, the O_{1s} band can be de-convoluted into two peaks located at approximately 530.2 and 531.8 eV, corresponding to Ti–O and Ti–O–N [4]. A typical de-convoluted O_{1s} band for sample N35 is presented in Fig. 3. The compositions of TiO_xN_y films were calculated using the XPS fitting results. The chemical formulas can be expressed as $TiO_{1.837}N_{0.060}$, $TiO_{1.890}N_{0.068}$, $TiO_{1.865}N_{0.073}$, and $TiO_{1.882}N_{0.163}$ for samples N2, N3, N35, and N4, respectively.

The electrical conductivities derived from the resistances are 1.8×10^{-5}, 1.2×10^{-4}, 2.1×10^{-4}, 2.8×10^{-4}, and 1.2×10^{-6} S/m for samples N0, N2, N3, N35, and N4, respectively. It is obvious that the conductivity of TiO_2 can be improved by introducing appropriate amount of nitrogen contents due to the semi-conducting behavior of

Download English Version:

https://daneshyari.com/en/article/1664499

Download Persian Version:

https://daneshyari.com/article/1664499

Daneshyari.com